

# Conductance of a SET with a retarded dielectric layer in the gate capacitor

O. G. Udalov,<sup>1,2</sup> N. M. Chtchelkatchev,<sup>3,4,5</sup> S. A. Fedorov,<sup>6</sup> and I. S. Beloborodov<sup>1</sup>

<sup>1</sup>*Department of Physics and Astronomy, California State University Northridge, Northridge, CA 91330, USA*

<sup>2</sup>*Institute for Physics of Microstructures, Russian Academy of Science, Nizhny Novgorod, 603950, Russia*

<sup>3</sup>*L.D. Landau Institute for Theoretical Physics, Russian Academy of Sciences, 117940 Moscow, Russia*

<sup>4</sup>*Department of Theoretical Physics, Moscow Institute of Physics and Technology, Moscow 141700, Russia*

<sup>5</sup>*Institute for High Pressure Physics, Russian Academy of Science, Troitsk 142190, Russia*

<sup>6</sup>*Department of Theoretical Physics, Moscow Institute of Physics and Technology, 141700 Moscow, Russia*

(Dated: July 14, 2021)

We study conductance of a single electron transistor (SET) with a ferroelectric (or dielectric) layer placed in the gate capacitor. We assume that ferroelectric (FE) has a retarded response with arbitrary relaxation time. We show that in the case of “fast” but still retarded response of the FE (dielectric) layer an additional contribution to the Coulomb blockade effect appears leading to the suppression of the SET conductance. We take into account fluctuations of the FE (dielectric) polarization using Monte-Carlo simulations. For “fast” FE these fluctuations partially suppress the additional Coulomb blockade effect. Using Monte-Carlo simulations we study the transition from “fast” to “slow” FE. For high temperatures the peak value of the SET conductance is almost independent of the FE relaxation time. For temperatures close to the FE Curie temperature the conductance peak value non-monotonically depends on the FE relaxation time. A maximum appears when the FE relaxation time is of the order of the SET discharging time. Below the Curie point the conductance peak value decreases with increasing the FE relaxation time. The conductance shows the hysteresis behavior for any FE relaxation time at temperatures below the FE transition point. We show that conductance hysteresis is robust against FE internal fluctuations.

PACS numbers: 75.70.-i 68.65.-k 77.55.-g 77.55.Nv

## I. INTRODUCTION

Single electron devices such as single electron transistors (SET), single electron (and Cooper pair) boxes, chains of metallic islands and etc., are currently in the focus of scientific interest due to their deep and complex physics and numerous promising applications [1–10]. One of the most interesting aspects of these systems is their dynamics. Due to charge quantization even DC current in a metallic chain of islands leads to a complicated dynamics and to the appearance of voltage oscillations similar to those existing in Josephson junctions [11, 12]. A great progress in fabrication of nanoscale metallic circuits allows creating of single electron devices coupled to nanomechanical resonators. In addition, SETs with moving metallic island exist. In these systems electrical and mechanical degrees of freedom are coupled leading to a complex dynamics of the whole device. SET with a mobile metal particle shows the “shuttling” effect [13–17]. Numerous groups studied SET with mobile gate electrode which has its own dynamics [10, 18–22]. Even a weak electro-mechanical coupling strongly influences the SET conductance promising very sensitive mechanical sensor. A strong electro-mechanical coupling causes bistability and hysteresis effects which are useful for memory applications.

Recently, a SET coupled to a ferroelectric (FE) layer was proposed and studied [23,24]. The FE layer can be placed either in the leads-island capacitors or in the gate capacitor. SET shows high sensitivity of conductivity to the FE dielectric properties. This allows to consider SET

as an effective way to study properties of nanosized FE materials. FE hysteresis in combination with its dynamics suggests that “turnstile” effect should exist in a SET with FE. This effect is the basis for a precise current standard [25].

When FE layer is placed in the tunneling junctions it serves as tunnel barriers for electrons, but the polarization of the FE layers have its own dynamics in contrast to the usual SET where the insulator polarization follows the electric field in the capacitors.

FE placed in the gate capacitor of SET (see Fig. 1(a)) also has its own dynamics. In this case the SET has much in common with SET having a mobile gate where movement of the electrode causes change of the gate induced charge. Variations of the FE polarization influence the SET in the similar way. However, there are several important differences between these two systems. Nanomechanical resonators are usually studied as linear oscillators. In contrast, the FE layer shows the non-linear response since the electric fields in the SET capacitors can exceed the FE saturation field [23,24]. Another important difference is related to the fact that the characteristic time scales of FE materials can be essentially lower than those of the nanomechanical systems and can be even comparable with characteristic times of SET. These characteristic timescales of FE layer and the SET determine the transport properties of the whole system.

Different kinds of FE materials show different dynamics. Shift type FEs are described by the second order (in time) differential equation [26]. These materials behave similar to oscillators with a certain resonant frequency  $\omega_0^{\text{FE}}$  (in the linear regime) and a damping time

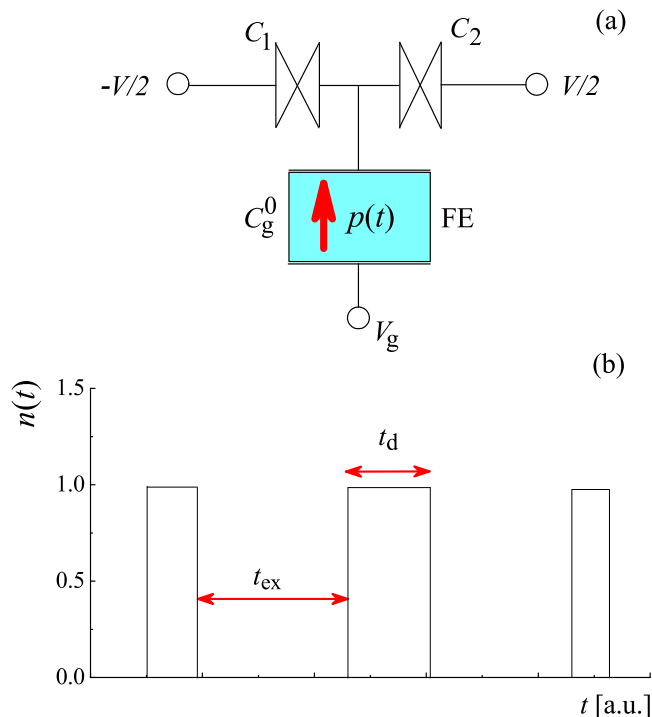


FIG. 1. (Color online) (a) Circuit diagram of SET coupled to a FE layer.  $C_{1,2}$  are the tunnel junctions capacitance,  $C_g^0$  is the geometrical gate capacitance,  $p(t)$  is the time-dependent polarization of the FE layer inside the gate capacitor,  $V$  and  $V_g$  are the bias and the gate voltages, respectively. (b) Number of excess electrons on the SET metal island  $n$  vs. time  $t$ . SET has the following characteristic times: the electron lifetime on the island (grain discharging time)  $t_d$  and the excitation time  $t_{ex}$ .

$t_{FE}$ . Order-disorder type FEs obey the first order differential equation. These materials are described by the damping time  $t_{FE}$  only.

The shortest timescale for SET is  $t_c \sim \hbar/E_c$ , where  $E_c$  is the charging energy. For a metallic grain of few nm this time is of order  $10^{-14}$  s. An intermediate timescale is the electron lifetime on the grain (grain discharging time),  $t_d \sim R C_\Sigma$ , where  $R$  and  $C_\Sigma$  are the resistance and the total capacitance of the system, respectively. This time depends on the geometry of the system and usually is in the range  $10^{-12}$ - $10^{-8}$  s. The longest time  $t_{ex}$  is the time between electron jumps to the grain. In general this time depends on the gate voltage. For strong Coulomb blockade it is exponentially large,  $t_{ex} \sim R C_\Sigma e^{E_c/T}$ , while for weak Coulomb blockade, due to applied gate voltage, it is comparable to the electron lifetime on the grain,  $t_d$ .

The limit,  $t_{FE} \ll t_c$ , corresponds to the “classical” theory of SET. In this case the polarization of insulators follows the electric field in the SET capacitors. When the grain charge changes from  $n$  to  $n \pm 1$  it is implicitly assumed that the polarization of insulators instantly changes from some equilibrium value  $p^{eq}|_n$  to different equilibrium value  $p^{eq}|_{n \pm 1}$ . Thus, the “classical” theory

of SET considers transitions between states  $(n, p^{eq}|_n)$  and  $(n \pm 1, p^{eq}|_{n \pm 1})$ .

The limit,  $t_{FE} \gg t_{ex}$ , was studied in Refs. [23,24] using the mean field theory. In this case the polarization of FE layers “feels” only the average electric field produced in the SET capacitors. The coupling of SET with slow dynamical system causes the hysteresis phenomena even in the absence of FE polarization hysteresis. In Ref. [27] the SET with “slow” dielectric in the gate capacitor was considered.

The region in between the limits discussed above can be divided into three subregions with the following boundaries: 1)  $t_{FE} \approx t_c$ ; 2)  $t_{FE} \approx t_d$ ; and 3)  $t_{FE} \approx t_{ex}$ . The first region requires consideration of a single tunneling event by taking into account the time dispersion of dielectric response. This case is beyond the orthodox theory. Next two regimes can be treated within the orthodox theory if polarization time dynamics is taken into account. In the present paper we consider the SET with dielectric or FE layer inside the gate capacitor with relaxation time larger than  $t_c$  ( $t_{FE} \gg t_c$ ) but with arbitrary ratio of  $t_{FE}$  and  $t_{d,ex}$ .

Two different methods are usually used to study dynamical effects in SET. The first approach calculates the probabilities of all possible states of the system using master equation [19,28]. These probabilities are time-dependent in general. This method is mostly used for investigation of SETs coupled to a mechanical nano resonator or with a mobile metal island. The mechanical subsystem can be treated classically [15, 17, 18, 21, and 22] or quantum-mechanically [14, 16, 20, 29, and 30]. The second approach simulates the time evolution of the whole system directly using the Monte-Carlo method [11,31]. This approach provides the complete information about SET behavior and allows to analyze time evolution of the system parameters. Currently a single electron counting is possible and time dependence of the metal island charge can be extracted from an experiment [32]. Therefore the results of Monte-Carlo simulations can be compared to a real experimental data.

In the present paper we use the Monte-Carlo simulations along with analytical consideration to study SET coupled to a FE layer behaving classically. In particular, we study the influence of the retarded response of the FE layer in the gate capacitor on the Coulomb blockade effects.

The paper is organized as follows. In Sec. II we describe the model of the SET with FE (dielectric) layer in the gate capacitor. In Sec. III we discuss our results: we consider analytically and numerically the SET conductance in the intermediate region  $t_c \ll t_{FE} \ll t_d$ . We discuss the evolution of the SET conductance with increasing the FE relaxation time from  $t_{FE} \ll t_d$  to  $t_{FE} \gg t_{ex}$ . We investigate the influence of the FE (dielectric) internal noise on the SET conductance.

## II. MODEL

We consider the SET shown in Fig. 1(a). Left and right electrodes (source and drain) are connected to a metallic island via tunnel junctions. The source and the drain are biased with voltage  $\pm V/2$ . For simplicity, we assume that all junctions have the same capacitances  $C_1 = C_2 = C/2$  and resistances  $R_1 = R_2 = R$ . An insulator with an instant response is placed inside the tunnel junctions. The polarization of the insulator instantly reacts to the electric field,  $p_{1,2} = \chi_{\text{jun}}(\pm V/2 - \phi)/d$ , where  $\phi$  is the grain potential,  $d$  is the junctions thickness and  $\chi_{\text{jun}}$  is the dielectric susceptibility of the insulator in the junctions. The polarizability of the tunnel barriers is incorporated into capacitances  $C_{1,2}$ . A gate electrode is capacitively coupled to the metallic island. A voltage  $V_g$  is applied to the electrode. The FE (dielectric) with retarded response is placed between the island and the gate. The characteristic time scale of the material,  $t_{\text{FE}}$ , is larger than  $t_c$ . We assume that the polarization  $p(t)$  of the FE (dielectric) layer in the gate capacitor is uniform and time dependent. We use the notation  $C_g^0 = S_g/(4\pi d_g)$  for geometrical capacitance of the gate-island capacitor, where  $S_g$  and  $d_g$  are the gate capacitor area and thickness, respectively.

Below we will distinguish two different temperatures: 1)  $T_{\text{FE}}$  is the FE layer temperature and 2)  $T_e$  is the leads and the island temperature. In general, these temperatures can be different on one hand due to the current flowing through the source-island-drain circuit which heats the island and the leads [33–35] and on the other hand different temperatures can be created artificially using local heating/cooling techniques. [36–39].

### A. Free energy of SET with FE (dielectric) layer in the gate capacitor

Equations governing the behavior of SET with a FE (dielectric) layer can be derived using the free energy of the system. The free energy increment can be expressed via charges  $q_i$  and potentials  $\phi_i$  of all the metallic electrodes  $\delta F = \delta R = \sum \phi_i \delta q_i$ . Here the charges are considered as independent variables. In a SET the three metallic electrodes are biased with a voltage source and the island potential should be found self-consistently. Following the standard approach [40] we introduce the thermodynamic potential where the island charge, the potentials of the leads and the gate potential are considered as independent variables  $\delta F_m = \delta F - \delta(V_g Q_g) - \delta(V_1 q_1) - \delta(V_2 q_2) = \phi \delta q - Q_g \delta V_g - q_1 \delta V_1 - q_2 \delta V_2$ , where  $Q_g$  is the charge of the gate electrode,  $q_{1,2}$  and  $V_{1,2}$  are the charges and the potentials of the leads,  $q$  and  $\phi$  are the metal island charge and potential, respectively. Below we use the notation  $F_m$  for free energy.

At zero bias voltage the increment of this mixed thermodynamic potential has the form  $\delta F_m = \phi \delta q - Q_g \delta V_g$ . Integration of  $\delta F_m$  over the  $\delta q$  and  $\delta V_g$  provides the total free energy. Using electrostatic consideration for the

charge at the gate electrode we find  $Q_g = (C C_g^0 V_g - q C_g^0 - p S_g C)/C_\Sigma$ , where  $C_\Sigma = C + C_g^0$  is the total capacitance of the system. The grain potential is given by  $\phi = (C_g^0 V_g + q - p S_g)/C_\Sigma$ . Thus,

$$F_m = F_0 + \frac{q^2}{2 C_\Sigma} + \frac{q C_g^0 V_g}{C_\Sigma} - \frac{p S_g q}{C_\Sigma} + \frac{p S_g C V_g}{C_\Sigma} - \frac{C C_g^0 V_g^2}{2 C_\Sigma}, \quad (1)$$

where  $F_0$  is the system free energy at zero gate voltage and zero grain charge

$$F_0 = (\alpha_P p^2/2 + \beta_P p^4/4 + p^2 S_g/(2 C_\Sigma d_g)) S_g d_g. \quad (2)$$

The first two terms in Eq. (2) are the usual contributions to the free energy describing the dielectric materials and FEs close to the paraelectric-ferroelectric phase transition [26]. Here  $\alpha_P$  and  $\beta_P$  are the phenomenological constants. For dielectric materials both constants are positive. For FEs the constant  $\alpha_P$  linearly depends on temperature and crosses zero at the FE phase transition point. The last term in Eq. (2) is due to the non-zero electric field  $E_0 = -4\pi C_g^0 p/C_\Sigma$  acting on the FE layer at  $q = 0$  and  $V_g = 0$ .

At finite bias voltage,  $V$ , the free energy  $F_m$  needs to be modified:  $F_m$  gets an additional contribution  $\pm eV/2$  when an electron is added to the grain.

For linear instant relation between the polarization  $p$  and the electric field,  $p(t) = \chi_0^i(\phi(t) - V_g)/d_g$ , we obtain the free energy of the SET with the properly renormalized capacitances  $C_g = C_g^0 \epsilon_0$  and  $C_\Sigma = C + C_g$ , where  $\epsilon_0 = 1 + 4\pi\chi_0^i$  is the effective dielectric constant of the layer in the gate capacitor.

### B. Ferroelectric dynamics

Varying the free energy in Eq. (1) with respect to the polarization  $p$  we find the equation governing  $p$ . Below we consider FEs (dielectrics) of the order-disorder type. These materials are described using the first order time dependent equation [26]

$$\gamma \dot{p} = -\frac{\partial F_m}{\partial p} + \tilde{\Gamma}_L, \quad (3)$$

where  $\gamma$  is the relaxation constant related to the relaxation time,  $t_{\text{FE}} = \gamma\chi_0$ , with  $\chi_0 = \alpha_P^{-1}$  being the linear response of the polarization to the external electric field.  $\tilde{\Gamma}_L$  describes an intrinsic noise of the FE layer. Substituting the free energy,  $F_m$ , into Eq. (3) we obtain the following non-linear equation for polarization

$$\gamma \dot{p} + \alpha_P p + \beta_P p^3 = \frac{q - C V_g - p S_g}{C_\Sigma d_g} + \tilde{\Gamma}_L. \quad (4)$$

We introduce the paraelectric-ferroelectric Curie temperature at which the coefficient in front of the linear term is zero,  $\chi^{-1} = \alpha_P + 4\pi C_g^0/C_\Sigma = \tilde{\alpha}_P(T_{\text{FE}} - T_C) = 0$ . We call the material inside the gate capacitor as a FE

material if the Curie temperature is positive  $T_C > 0$ . For  $T_{\text{FE}} > T_C$ , Eq. (4) has only one solution, while for  $T_{\text{FE}} < T_C$  the spontaneous polarization appears leading to multiple solutions of the equation.

Another Curie temperature  $T_C^0$  can be introduced using the relation  $\chi_0^{-1} = \tilde{\alpha}_P^0(T_{\text{FE}} - T_C^0) = 0$ . It corresponds to the same FE but confined by the shorted metal electrodes. One can see that  $T_C < T_C^0$ . When a FE is placed in between the shorted metal electrodes the potential difference and the electric field are fixed across the FE layer. In contrast, in SET problem the potential of the metal island should be found self-consistently. Therefore the equation governing the FE layer gives the lower Curie temperature. Physically this reflects the fact that the depolarizing electric field inside the FE layer is not fully screened by the metal island in the SET. This complicates the appearance of the spontaneous polarization.

We notice that  $\chi_0$  is the susceptibility of the FE (dielectric) layer with respect to the external electric field, while  $\chi$  is the susceptibility with respect to the external charges  $q$  and  $Q_0 = -C_g^0 V_g$ . Below we will refer to  $Q_0$  as the gate charge. However,  $Q_0$  is not the real charge at the gate electrode and it differs from  $Q_g$  which was introduced above. For  $T_{\text{FE}} > T_C$  two susceptibilities  $\chi$  and  $\chi_0$  are related as follows  $\chi^{-1} = \chi_0^{-1} + 4\pi C_g^0 / C_\Sigma$ . For FE (dielectric) materials with instant response the constant  $\chi_0$  defines the dielectric permittivity,  $\chi_0^1 = \chi_0$  and  $\epsilon_0 = 1 + 4\pi\chi_0$ .

We regard the material in the gate capacitor as a dielectric if the quantity,  $\alpha_P + 4\pi C_g^0 / C_\Sigma > 0$ , is positive for any temperature. In general, we can consider the dielectric material as the material with the negative Curie temperature,  $T_C < 0$ .

In our Monte-Carlo simulations we solve the non-linear Eq. (4) directly. For analytical consideration at temperatures  $T_{\text{FE}} > T_C^0$  we linearize Eq. (4)

$$\gamma \dot{q}_P + \chi^{-1} q_P = \frac{4\pi C_g^0 (q - C V_g)}{C_\Sigma} + \Gamma_L. \quad (5)$$

Here we introduce the charge  $q_P = p S_g$  and  $\Gamma_L = S_g \tilde{\Gamma}_L$ .

We mention that below  $T_C^0$  the susceptibility  $\chi_0$  becomes negative. However, the FE layer is still in the paraelectric phase for temperatures  $T_C < T_{\text{FE}} < T_C^0$ . We show that in this temperature region Eq. (5) is not valid since it produces divergent solutions for  $q_P$  and  $q$ . The nonlinear term  $\beta_P p^3$  should be taken into account to restrict variations of  $q_P$  and  $q$ .

### C. Langevin forces

Internal fluctuations of the FE layer occur due to the interaction of FE (dielectric) polarization with all other degrees of freedom in the FE layer. This interaction has two components. The ‘‘regular’’ component leads to the appearance of polarization relaxation. This

term can be written in the form  $\gamma \dot{q}_P$  even for nonlinear systems [41]. Another noise component is responsible for fluctuations of the FE layer polarization. It appears in the RHS of Eq. (4) as a random Langevin force  $\tilde{\Gamma}_L$ . If polarization varies slowly in time in comparison to characteristic time of internal FE processes the correlation function of the Langevin forces can be chosen as  $C_L = \langle \tilde{\Gamma}_L(t) \tilde{\Gamma}_L(t') \rangle = 2\gamma k_B T_{\text{FE}} \delta(t - t') / (S_g d_g)$ . The relation between the relaxation constant  $\gamma$  and the Langevin forces dispersion is valid even for nonlinear systems [41]. The dispersion of the polarization fluctuations in the linear response regime ( $\beta_P \ll \alpha_P p^2$ ) can be written using the FE layer susceptibility as follows  $D_P = \langle (\Delta p)^2 \rangle = \chi k_B T_{\text{FE}} / (S_g d_g)$ . Below we will use this expression for estimates. For strong nonlinear effects ( $\beta_P \sim \alpha_P p^2$ ) the polarization dispersion is given by more complicated expression [42].

### D. SET dynamics

The probability of electron hop to/from the metallic island is given by the expression

$$G_{1,2}^\pm = \frac{1}{e^2 R} \frac{\Delta F_{1,2}^\pm}{e \Delta F_{1,2}^\pm / T_e - 1}, \quad (6)$$

where

$$\begin{aligned} \Delta F_1^\pm &= 2E_c \left( \pm \left( n + \frac{C_g^0 V_g}{e} + \frac{C_\Sigma V}{2e} - \frac{q_P}{e} \right) + 1/2 \right), \\ \Delta F_2^\pm &= 2E_c \left( \pm \left( n + \frac{C_g^0 V_g}{e} - \frac{C_\Sigma V}{2e} - \frac{q_P}{e} \right) + 1/2 \right). \end{aligned} \quad (7)$$

Subscript (1,2) denotes the electrode from which (or to which) an electron jumps. Superscript + describes electron hopping from a certain lead to the particle. Superscript - describes electron hopping from the island to a certain lead.  $n = q/e$  is the island population.  $E_c = e^2 / (2 C_\Sigma)$  is the bare charging energy.

Important assumption made when calculating  $\Delta F$  is that polarization  $p$  does not change during the electron hop since  $t_{\text{FE}} \gg t_c$ . Equation (7) describes the processes  $(n, p(t)) \rightarrow (n \pm 1, p(t))$ . This is in contrast to the ‘‘classical’’ SET situation where polarization  $p$  adjusts during the hop and the following processes occur  $(n, p^{\text{eq}}|_n) \rightarrow (n \pm 1, p^{\text{eq}}|_{n \pm 1})$ .

Two characteristic times can be introduced using Eq. (6): 1) the excitation time  $t_{\text{ex}}$  corresponding to the island charging event at zero gate voltage,  $V_g = 0$ . This event is suppressed due to Coulomb blockade effect,  $t_{\text{ex}} = G_1^+|_{n=0, V_g=0, q_P=0, V=0} \sim R C_\Sigma e^{E_c/T_e}$ ; 2) the relaxation time  $t_d$  corresponding to the discharging of the charged island. This time is much shorter,  $t_{\text{ex}} \gg t_d$ , since there is no exponential factor in this case,  $t_d = G_1^-|_{n=1, V_g=0, q_P=0, V=0} \sim R C_\Sigma$ . We mention that

excitation time depends strongly on the gate voltage  $V_g$ . And for certain voltages both times are comparable.

The island population is defined by the random electron jumps from and to the island

$$\dot{n}(t) = \sum_i Z_i \delta(t - t_i). \quad (8)$$

Here  $Z_i$  has three possible values  $\pm 1$  and 0. The probability for electron to hop per unit time is defined by Eq. (6). It depends on the bias voltage  $V$ , the gate voltage  $V_g$ , the number of electrons on the island  $n(t)$  and the FE layer induced charge  $q_p(t)$ . The last two quantities depend on time leading to time dependent hopping probabilities. Thus, one has to solve self-consistent equations for the FE layer and the SET.

We use numerical Monte-Carlo simulations [11] to solve coupled SET and FE equations. Equation (8) can be written in the discrete form

$$\begin{aligned} n(t_i) &= n(t_{i-1}) + Z(n(t_{i-1}), q_p(t_{i-1}))dt, \\ Z &= \begin{cases} 1, & x < G_1^+ + G_2^+, \\ 0, & G_1^+ + G_2^+ < x < 1 - (G_1^- + G_2^-), \\ -1, & x > 1 - (G_1^- + G_2^-), \end{cases} \end{aligned} \quad (9)$$

where  $x$  is the random value uniformly distributed between 0 and 1,  $dt = t_i - t_{i-1}$ . The time interval  $dt$  is much shorter than all characteristic times in the problem,  $dt \ll t_d, t_{FE}$ .

The average electric current through the SET can be calculated as follows

$$\begin{aligned} I &= \frac{e}{T_m} \sum_i \zeta(t_i), \\ \zeta &= \begin{cases} 1, & Z(t_i) > 0 \wedge y < G_1^+ / (G_1^+ + G_2^+), \\ -1, & Z(t_i) < 0 \wedge y < G_1^- / (G_1^- + G_2^-), \\ 0, & Z(t_i) = 0, \end{cases} \end{aligned} \quad (10)$$

where  $y$  is the random number uniformly distributed between 0 and 1;  $T_m$  is the measurement time interval.

### III. CONDUCTANCE OF SET WITH RETARDED FE (DIELECTRIC) LAYER

We investigate the behavior of SET conductance as a function of gate voltage,  $V_g$  for different ratios of the FE (dielectric) relaxation time,  $t_{FE}$ , and SET characteristic times  $t_{ex}$  and  $t_d$ .

#### A. Suppression of Coulomb blockade due to internal noise of FE

The conductance peaks as a function of gate charge  $Q_0$  have a finite width at finite temperatures. The width of these peaks is defined as  $\Delta Q_0^L \approx ek_B T_e / E_c$ . The polarization of the FE (dielectric) layer enters the SET

equations as an additional gate capacitor charge. Therefore the FE (dielectric) polarization fluctuations can be considered as fluctuations of the gate charge  $Q_0$ . These fluctuations average the SET conductance over the region  $\Delta Q_0^p \sim \sqrt{D_p} \sim \sqrt{T_{FE}}$ . Due to the square root dependence of  $\Delta Q_0^p$  on temperature, the internal fluctuations of the FE polarization produce much stronger effect on the conductance than the finite temperature of the leads. If temperature of the FE layer  $T_{FE}$  equals to the source and drain electrodes temperatures,  $T_e$ , then the FE fluctuations are negligible for temperatures  $k_B T_{FE} \ll 2\pi\chi C_g^0 E_c / C_\Sigma$ . Also, FE fluctuations can be neglected for temperatures,  $T_{FE} \ll T_e$ .

If  $\Delta Q_0^p$  exceeds the half of an electron charge the Coulomb blockade effect is smeared and the conductance peaks as a function of the gate voltage disappear. Thus, the general condition for observation of charge quantization effects relates the polarization dispersion and the electron charge,  $S_g \sqrt{D_p} \ll e/2$ .

Below we show that FE fluctuations can increase the SET conductance in some cases.

#### B. SET with “instant” FE (dielectric) in the gate capacitor

We call FEs (dielectrics) with  $t_{FE} \ll t_c$  as FEs (dielectrics) with instant response, for brevity we call them “instant” FEs (dielectrics). In contrast, we call FEs “retarded” if  $t_{FE} \gg t_c$ . A SET with “instant” dielectrics was studied in many papers using the orthodox theory. In this case the conductance is a periodic function of the gate charge  $Q_0$ . The conductance maxima are located at points  $Q_0 = e(l + 1/2)/\epsilon_0$ , where  $l$  is an integer number. The peak value of the SET conductance in this case is  $\sigma_0 = 1/(4R)$ . The conductance is suppressed between peaks due to the Coulomb blockade effect.

If SET is coupled to a FE with relaxation time  $t_{FE} \approx t_c$ , the SET can not be studied within the orthodox theory. This case requires the calculation of tunneling matrix elements of electrons interacting with FE (dielectric) polarization varying on time scale  $t_c$ . Tunneling in the presence of time dispersion was considered in the past [43–45]. It was shown that time dispersion, caused by the dissipation in the tunnel junction circuit, leads to the decrease of the junction conductance and to the appearance of an effective Coulomb blockade effect.

#### C. SET with “fast” FE (dielectric) in the gate capacitor ( $t_{FE} \ll t_d$ )

In the case of “fast” FE (dielectric),  $t_c \ll t_{FE} \ll t_d$ , each electron jump to the grain or out of grain occurs when polarization is in it’s equilibrium state at a given grain population  $n$ . However, during the jump the FE (dielectric) polarization preserves it’s value since  $t_{FE} \gg t_c$ , meaning that the state of the FE polarization

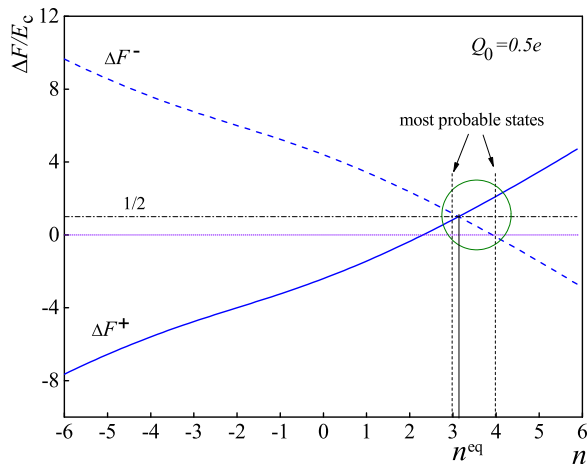


FIG. 2. (Color online) Free energy difference, Eq. (7), at  $V = 0$  and  $Q_0 = 0.5e$  vs.  $n$ . Solid line shows  $\Delta F^+(n)$ , dashed line shows  $\Delta F^-(n)$ . Intersection of  $\Delta F^+$  and  $\Delta F^-$  shows the most probable state of the SET at a given  $Q_0$ .

is not equilibrium after the jump. We define the state of the SET at each moment with the pair  $(n(t), p(t))$ . The following transitions correspond to the events of grain charging and discharging  $(n, p|_n^{\text{eq}}) \rightarrow (n \pm 1, p|_{n \pm 1}^{\text{eq}})$ , where  $p|_n^{\text{eq}}$  stands for equilibrium polarization at given  $n$  and  $Q_0$

$$\chi^{-1} p^{\text{eq}}|_n + \beta_{\text{P}} (p^{\text{eq}}|_n)^3 = \frac{en + CQ_0 / C_{\text{g}}^0}{C_{\Sigma} d_{\text{g}}}. \quad (11)$$

We mention that for SET with “instant” insulators different kind of transitions occur  $(n, p|_n^{\text{eq}}) \rightarrow (n \pm 1, p|_{n \pm 1}^{\text{eq}})$ .

Consider the free energy difference in Eq. (7) as a function of island population  $n$  at  $V = 0$ . The stable population of the island is approximately defined by the conditions

$$\begin{cases} \Delta F^+(n+1, p^{\text{eq}}|_{n+1}) > \Delta F^-(n+1, p^{\text{eq}}|_{n+1}), \\ \Delta F^+(n, p^{\text{eq}}|_n) < \Delta F^-(n, p^{\text{eq}}|_n). \end{cases} \quad (12)$$

We find approximately the “equilibrium” value of  $n$  and polarization  $p$  at a given value of  $Q_0$  using the following equation

$$\Delta F^+(n^{\text{eq}}, p^{\text{eq}}|_{n^{\text{eq}}}) = \Delta F^-(n^{\text{eq}}, p^{\text{eq}}|_{n^{\text{eq}}}). \quad (13)$$

Here  $n^{\text{eq}}$  stands for approximately the most probable population of the island, it may have a non-integer value. Equation (13) can be rewritten in the form

$$en^{\text{eq}} - Q_0 - q_{\text{P}}^{\text{eq}}|_{n^{\text{eq}}} = 0, \quad (14)$$

where  $q_{\text{P}}^{\text{eq}}|_{n^{\text{eq}}} = S_{\text{g}} p^{\text{eq}}|_{n^{\text{eq}}}$ . Using Eq. (11) we can relate the “equilibrium” polarization and the gate charge  $Q_0$

$$\alpha_{\text{P}} (q_{\text{P}}^{\text{eq}}|_{n^{\text{eq}}}) + \tilde{\beta}_{\text{P}} (q_{\text{P}}^{\text{eq}}|_{n^{\text{eq}}})^3 = 4\pi Q_0, \quad (15)$$

where  $\tilde{\beta}_{\text{P}} = \beta_{\text{P}} / S_{\text{g}}^2$ . Equation (15) has a unique solution for temperatures  $T_{\text{FE}} > T_{\text{C}}^0$ . For  $T_{\text{FE}} < T_{\text{C}}^0$  it has three

different solutions. Introducing  $p^{\text{eq}}|_{n^{\text{eq}}}$  into Eq. (14) we find the “equilibrium” population  $n^{\text{eq}}$ . At a given  $Q_0$  the whole system state most probably will be in the vicinity of  $n^{\text{eq}}$ . To find approximately the SET conductance we take into account only two states  $n_1$  and  $n_2$  ( $n_1 < n_2$ ) nearest to  $n^{\text{eq}}$ . Using the expression

$$\sigma = \frac{e}{V} \frac{\tilde{G}_2^+ \tilde{G}_1^- - \tilde{G}_1^+ \tilde{G}_2^-}{\tilde{G}_1^+ + \tilde{G}_2^+ + \tilde{G}_1^- + \tilde{G}_2^-} \quad (16)$$

we find the SET conductance. We use the following notations in Eq. (16):  $\tilde{G}_{1,2}^+ = G_{1,2}^+|_{n=n_1}$ ,  $\tilde{G}_{1,2}^- = G_{1,2}^-|_{n=n_2}$ . Below we consider the behavior of SET conductance at different temperatures.

### 1. $T_{\text{FE}} > T_{\text{C}}^0$ .

In this temperature region the parameter  $\alpha_{\text{P}}$  is positive and Eq. (15) has only one solution leading to one “stable” state for a whole system. Figure 2 shows the free energy difference as a function of the island population  $n$  for  $C_{\text{g}}^0 = 0.2 C_{\Sigma}$ ,  $\alpha_{\text{P}} = 1.5$ ,  $e^2 \tilde{\beta}_{\text{P}} = 0.13$  and  $Q_0 = 0.5e$ . Inequalities (12) are satisfied for  $n = 3$  only. Equation (15) gives the “equilibrium” population  $n^{\text{eq}}$  slightly higher than 3. The most probable states are  $n = 3$  and  $n = 4$ . Figure 3 shows the SET conductance (Eq. (16)) as a function of the gate charge  $Q_0$  for parameters  $C_{\text{g}}^0 = 0.005 C_{\Sigma}$ ,  $\alpha_{\text{P}} = 0.12$ ,  $e^2 \tilde{\beta}_{\text{P}} = 0.0013$ , and  $T_{\text{e}} = 0.2 E_{\text{c}}$ . These parameters correspond to TTF-CA FE at  $T_{\text{FE}} = 120$  K [46]. This FE has rather small relaxation time in the ps region [47], which can be comparable, smaller or larger than discharging time of SET. The conductance appears as series of peaks. The period and the height of the peaks are not constant due to nonlinear term in Eq. (4). The red circle shows the typical region where Eq. (16) is not valid. In this region at least three states are involved into electron transport, whereas Eq. (16) accounts for only two states. The dashed line shows the conductance calculated using numerical Monte-Carlo (MC) simulations. We use  $\gamma = 0.05 R C_{\Sigma}$ . The numerical and analytical results coincide in the vicinity of the conductance peaks, where Eq. (16) works well. Close to the conductance deeps the numerical result is more accurate since all possible states are taken into account in the simulations. The conductance peaks value is smaller than  $\sigma_0$  for “fast” FE. Below we show that this is a consequence of an effective additional Coulomb blockade appearing due to the retarded response of the FE layer.

It is important that Eq. (16) does not take into account internal fluctuations of the FE polarization. This approximation is valid, for example, for temperatures  $T_{\text{FE}} \ll T_{\text{e}}$ . To fit blue curve in Fig. 3 with MC simulations we turned off the Langevin forces in Eq. (4). The result is the red dashed line.

The dotted black line in Fig. 3 shows the result of MC modelling for  $T_{\text{FE}} = T_{\text{e}}$  in the presence of FE internal fluctuations. One can see that the FE fluctuations are important for electron transport. The internal fluctuations

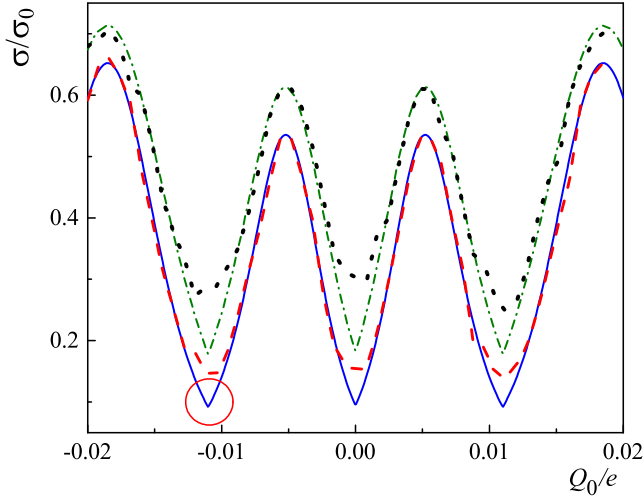


FIG. 3. (Color online) SET conductance vs. the gate charge  $Q_0$  for temperatures  $T_{\text{FE}} > T_C^0$ . Solid blue line is calculated using Eq. (16) at electron temperature  $T_e = 0.2E_c$ . Dashed red line and dotted black line are obtained using MC simulations. Dashed line is calculated in the absence of FE internal fluctuations. Dotted black line is calculated in the presence of fluctuations. Green dash dotted line is calculated with Eq. (16) at  $T_e = 0.26E_c$ . Red circle shows the typical region where Eq. (16) is not valid.

suppress the additional Coulomb blockade increasing the conductance. For comparison we show the conductance calculated using Eq. (16) for the same SET parameters but with higher electron temperature,  $T_e = 0.26 E_c$  (dash dotted green line).

For small enough parameter  $\beta_P$  we can neglect non-linear effects and use the linearized equation for the FE polarization, Eq. (5). In this case the SET conductance is a periodic function of parameter  $Q_0$  with the period  $\Delta Q_0 = e/\epsilon_0$ . Consider the conductance in the vicinity of the first peak position  $Q_0 = -e/(2\epsilon_0)$ . Figure 4 shows different processes contributing to the electron transport of the SET with “retarded” FE layer. This figure shows a number of branches of the SET free energy as a function of the gate charge  $Q_0$ . These branches correspond to the island population  $n = 0, 1$  and the FE polarization  $p^{\text{eq}}|_{0,1}$ . For SET with “retarded” FE the transitions (charging and discharging events) occur between the states with non-equilibrium polarization of the FE (dielectric) layer. This leads to the appearance of a non-zero energy gap (see Fig. 4) for any gate voltage. Such a gap can be considered as an additional effective Coulomb blockade appearing due to “retarded” FE (dielectric) response.

At  $\epsilon_0 Q_0 = e/2$  the charging event  $(0, p|_0^{\text{eq}}) \rightarrow (1, p|_0^{\text{eq}})$  (process (1) in Fig. 4) requires an additional energy  $\Delta F_0 = 4\pi\chi C_g^0 E_c / C_\Sigma$ . The FE layer relaxes to its equilibrium state  $p|_1^{\text{eq}}$  (the process (2) in Fig. 4) after the grain charging event. The discharging process (3)  $(1, p|_1^{\text{eq}}) \rightarrow (0, p|_1^{\text{eq}})$  is also inelastic. It requires the same

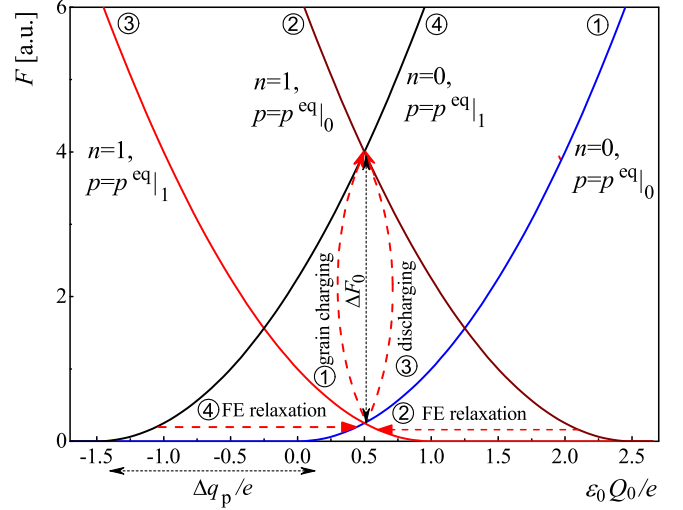


FIG. 4. (Color online) Free energy as a function of gate charge  $Q_0$ . Blue branch (1) corresponds to the state  $(0, p^{\text{eq}}|_0)$ , red branch (3) corresponds to the state  $(1, p^{\text{eq}}|_1)$ , brown branch (2) shows the free energy for the state  $(1, p^{\text{eq}}|_0)$  and black branch (4) shows the free energy for the state  $(0, p^{\text{eq}}|_1)$ . At  $\epsilon_0 Q_0 = e/2$  in the SET with “instant” insulators the grain charging and discharging events correspond to the transition from blue to the red branch. Energy gap in this case is zero leading to large conductance. For SET with “retarded” FE another kind of transitions occurs. The island charging event (1) corresponds to the transition from blue branch (1) to the brown branch (2). After the transition the FE polarization relaxes to a new equilibrium state (process depicted by the horizontal arrow (2)). The grain discharging event (3) corresponds to the transition from red (3) to the black (4) branch. Finally, the FE polarization relaxes again (process (4)).  $\Delta F_0 = 4\pi\chi C_g^0 E_c / C_\Sigma$ ,  $\Delta q_P = (4\pi\chi C_g^0 / C_\Sigma)e$ .

energy  $\Delta F_0$ . This energy gap suppresses the conductance of the SET with “retarded” FE layer. For SET with “instant” FE (dielectric) layer the charging and discharging transitions occur directly from branch (1) to branch (3) and do not require any energy at  $\epsilon_0 Q_0 = e/2$  leading to a higher conductance.

For temperatures  $T_e \ll E_c(4\pi\chi C_g^0 / C_\Sigma)$  the maximum conductance value is

$$\sigma_{\text{max}} \approx \frac{1}{R} \frac{2\pi\chi C_g^0 E_c}{C_\Sigma T_e} e^{-\frac{\Delta F_0}{T_e}}. \quad (17)$$

The magnitude of conductance peak increases exponentially with temperature, however it stays smaller than the “classical” value of SET conductance  $\sigma_0$ . We mention that for SET with “instant” insulators the magnitude of conductance peak is temperature independent.

$$2. \quad T_C < T_{\text{FE}} < T_C^0$$

In this temperature region the susceptibility  $\chi_0$  is negative and Eq. (15) has three different solutions mean-



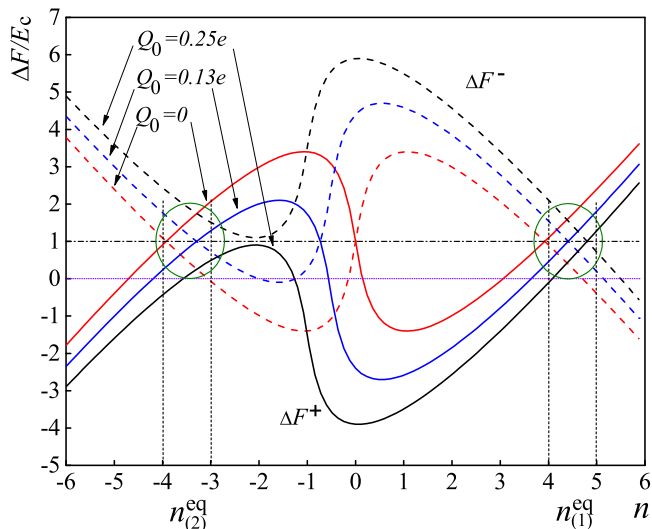


FIG. 5. (Color online) Free energy difference, Eq. (7), at  $V = 0$  vs.  $n$ . Solid lines show  $\Delta F^+(n, p^{\text{eq}}|_n)$ , dashed lines show  $\Delta F^-(n, p^{\text{eq}}|_n)$ . Red lines correspond to  $Q_0 = 0$ , blue lines show  $\Delta F^\pm$  at  $Q_0 = 0.13e$  and black lines show the case of  $Q_0 = 0.25e$ . Negative  $\chi_0$  provides the negative slope of  $\Delta F^+$  and positive slope of  $\Delta F^-$  in the vicinity of  $n = 0$ .

ing that there are more than one stable state in the whole SET system. Figure 5 shows  $\Delta F^\pm(n, p^{\text{eq}}|_n)$  for different  $Q_0$  for the following SET parameters  $\alpha_P = -2$ ,  $\chi^{-1} = 0.513$ ,  $e^2\tilde{\beta}_P = 0.13$ ,  $C_g^0 = 0.2 C_\Sigma$ .

Here the dependencies are non-monotonic in contrast to the case  $T_{\text{FE}} > T_C^0$ . Consider the blue curves corresponding to  $Q_0 = 0.13e$ . One can see that the state with zero island population is not stable. Two stable states, shown by the green circles, occur in the vicinity of  $n_{(1)}^{\text{eq}} \approx 4.5e$  and  $n_{(2)}^{\text{eq}} \approx -3.5e$ . Depending on the initial system state both “equilibrium” populations can be realized. In this case one can expect the hysteresis behavior of the SET conductance as a function of the gate voltage. Figure 5 shows that for high enough gate voltage (black lines) only one stable state remains meaning that conductance hysteresis exists only around  $Q_0 = 0$ . This is in contrast to the case of SET with “slow” FE considered in Refs. [23,24], where hysteresis appears in the vicinity of each conductance peak. The nature of hysteresis in the case of “slow” FE in the gate capacitor is very different from the case of “fast” FE (dielectric). For “fast” FE the hysteresis is related to the instability ( $\chi_0 < 0$ ) of the FE dielectric properties, while for “slow” FE the hysteresis occurs even in the absence of FE instability due to the interaction of the fast SET system with the slow FE layer.

Note that in the region  $T_C < T_{\text{FE}} < T_C^0$  the nonlinear term in Eq. (4) for the FE polarization can not be neglected since the population  $n(t)$  and the polarization  $p(t)$  will be divergent functions.

Figure 6 shows the SET conductance as a function of the gate charge  $Q_0$  for the following parameters:  $\alpha_P =$

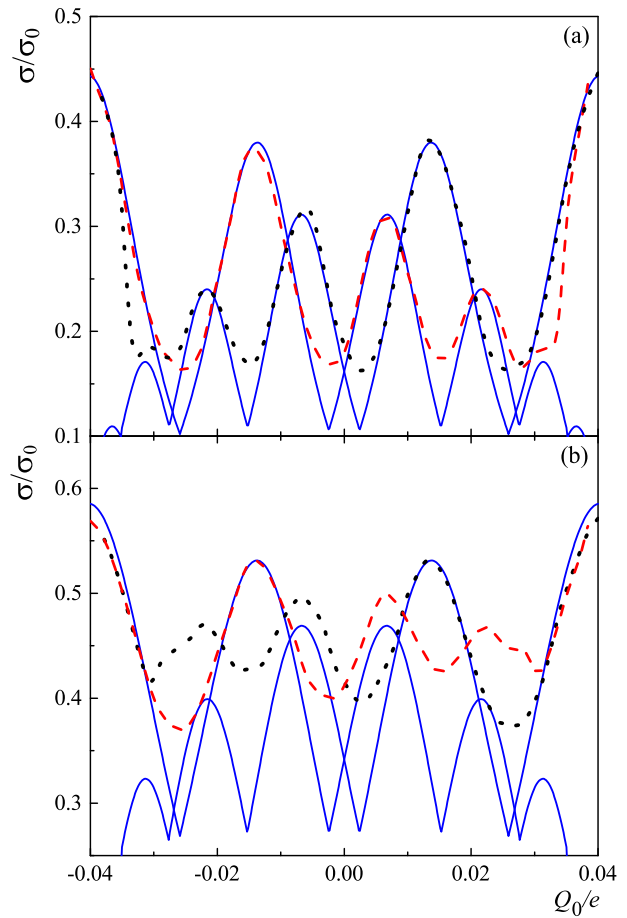


FIG. 6. (Color online) Conductance of SET as a function of gate charge  $Q_0$  for temperatures  $T_C < T_{\text{FE}} < T_C^0$ . Solid blue lines are calculated using Eq. (16). In the vicinity of  $Q_0 = 0$  there are two branches of the conductance due to the SET instability. Dashed red line and dotted black line are calculated using MC simulations. Dashed line is obtained for increasing parameter  $Q_0$  during simulations, while the dotted line is obtained for decreasing  $Q_0$ . Panel (a) shows results obtained using Eq. (16) at  $T_e = 0.2E_c$  and results of MC simulations at  $T_e = 0.2E_c$  in the absence of FE internal fluctuations. Panel (b) shows results obtained using Eq. (16) at  $T_e = 0.3E_c$  and results of MC simulations in the presence of FE internal fluctuations and at  $T_e = 0.2E_c$ .

$-0.12$ ,  $e^2\tilde{\beta}_P = 0.0013$ ,  $C_g^0 = 0.02 C_\Sigma$ . These parameters correspond to TTF-CA FE at  $T_{\text{FE}} \approx 50$  K [46]. Solid lines demonstrate the result obtained using Eq. (16) at  $T_e = 0.2E_c$  (panel (a)) and  $T_e = 0.3E_c$  (panel (b)). One can see that there are two branches of the conductance as a function of the gate voltage. Dashed and dotted lines demonstrate the conductance obtained using MC simulations in the absence of FE internal fluctuations (panel (a)) and in the presence of fluctuations (panel (b)). To obtain the red dashed lines we increase  $Q_0$  from  $-0.5e$  to  $+0.5e$ . The initial polarization and the island population at each  $Q_0$  were taken from the last simulation point at previous  $Q_0$ . Dotted lines correspond to the



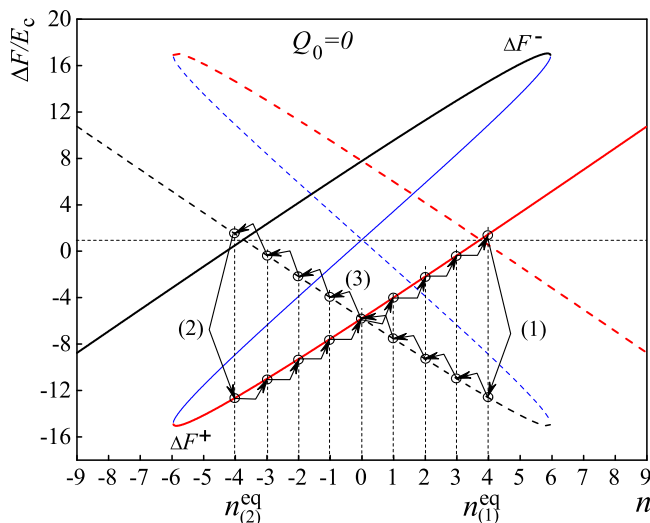


FIG. 7. (Color online) Free energy difference, Eq. (7), at  $V = 0$  and  $Q_0 = 0$  vs.  $n$ . Solid lines show  $\Delta F^+(n, p_{1,2}^{\text{eq}}|n)$ , dashed lines show  $\Delta F^-(n, p_{1,2}^{\text{eq}}|n)$ . Various colors correspond to different FE layer polarization states. Blue lines show the unstable polarization state,  $p_3^{\text{eq}}|n$ , which can not be realized in an experiment. Red line stands for positive polarization, black line corresponds to negative polarization. Black arrows show possible behavior of the SET.

case of decreasing  $Q_0$ . MC simulations confirm the existence of the conductance hysteresis. The analytical and numerical curves agree well with each other. Part of the conductance branches, for example between  $Q_0 = 0.1e$  and  $Q_0 = 0.25e$ , obtained using Eq. (16) is not realized in numerical simulations within the chosen protocol. To observe these branches we need to set a special initial conditions in our system which is hard to realize in an experiment.

Panel (b) shows the result of simulations in the presence of FE internal fluctuations ( $T_{\text{FE}} = T_e$ ). One can see that fluctuations suppress the Coulomb blockade and increase the conductivity. The peak positions stay the same. The FE fluctuations at given parameters do not smear the hysteresis.

### 3. $T_{\text{FE}} < T_C$

In this region the solution of Eq. (4) becomes ambiguous leading to a more complicated behavior of the SET. Two different equilibrium polarizations  $p_{1,2}^{\text{eq}}|n$  correspond to a single island population value  $n$ . Consider the free energy difference as a function of  $n$  at  $\alpha_P = -7$ ,  $e^2\tilde{\beta}_P = 0.5$ ,  $C_g^0 = 0.1 C_\Sigma$ ,  $Q_0 = 0$  (Fig. 7). Quantities  $\Delta F^\pm$  have two branches depicted by red and black curves. These branches correspond to equilibrium polarization states  $p_1^{\text{eq}}|n$  and  $p_2^{\text{eq}}|n$ . Blue lines show unstable solutions. “Equilibrium” population  $n_{(1)}^{\text{eq}}$  is defined by the intersection of two red lines. In contrast to the

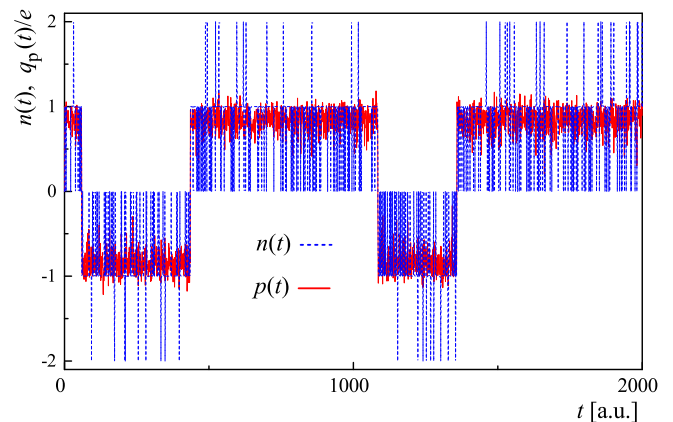


FIG. 8. (Color online) Island population  $n$  (blue dashed line) and FE layer induced charge,  $q_p/e$ , (red solid line) vs. time  $t$  for the following parameters  $\alpha_P = -0.15$ ,  $e^2\tilde{\beta}_P = 0.2$ ,  $C_g^0 = 0.002 C_\Sigma$ ,  $Q_0 = 0$ . The FE layer polarization switches between two equilibrium states due to thermal fluctuations.

case of  $T_{\text{FE}} > T_C$ , there is an additional allowed state at  $n = n_{(1)}^{\text{eq}}$  corresponding to another FE polarization. Due to inequalities (12) this second state is unstable with respect to variations of  $n$ . The internal fluctuations of the FE polarization may cause switching of the polarization (process (1) in Fig. 7) leading to the transition to another “equilibrium” population state  $n_{(2)}^{\text{eq}}$ . We depict a possible dynamical process in the SET in Fig. 7 by the black arrows. The system switches back and forth between two population states,  $n = n_{(1)}^{\text{eq}}$  and  $n = n_{(2)}^{\text{eq}}$ .

The temperature driven transition between two FE equilibrium polarization states is defined by the energy barrier between these two states, which can be estimated as  $\Delta W_p \approx 2S_g d_g \alpha_P^2 / (\beta_p) = 2\alpha_P^2 / (4\pi\tilde{\beta} C_g^0)$ . Varying parameters one can make this barrier much higher than  $E_c$ , thus prohibiting the polarization switching. In this case there is no population “wandering” and the whole system behaves similarly to the case of  $T_{\text{FE}} > T_C$ . In particular, the conductance shows hysteresis as a function of  $Q_0$ . For parameters used in Fig. 7,  $\Delta W_p > 100E_c$ . Therefore processes (1) and (2) are almost prohibited. The hysteresis behavior in the system with above parameters is rather robust.

The hysteresis can also be smeared through the consecutive change of  $n$ . The transition between  $n = n_{(1)}^{\text{eq}}$  and  $n = n_{(2)}^{\text{eq}}$  through such changes requires at least energy of order  $16E_c$ . This estimate is obtained using Fig. 7 as a maximum value of the red dashed curve. Moreover, the SET should go through several transitions  $(n) \rightarrow (n-1)$  to reach the equilibrium state  $n = n_{(1)}^{\text{eq}}$  from  $n = n_{(2)}^{\text{eq}}$ . Thus, the probability of such a switching between equilibrium states is negligible.

For barrier  $\Delta W_p \sim k_B T_{\text{FE}}$  the system switches between states  $n = n_{(1)}^{\text{eq}}$  and  $n = n_{(2)}^{\text{eq}}$ . This behavior is shown in Fig. 8 where we depict functions  $n(t)$  and  $p(t)$  obtained using MC simulation with the following

parameters  $\alpha_P = -0.15$ ,  $e^2\tilde{\beta}_P = 0.2$ ,  $C_g^0 = 0.002 C_\Sigma$ ,  $Q_0 = 0$ . Our MC simulations show that in this case there is no hysteresis behavior of the conductance as function of  $Q_0$ . This happens because the switching between different polarization states  $p_{1,2}^{\text{eq}}|n$  means that on the long time scale the FE layer behaves as a paraelectric layer due to strong fluctuations. Note that such a mechanism of hysteresis suppression does not exist for temperatures  $T_C < T_{\text{FE}} < T_C^0$ . In this region the polarization  $p$  has always a single value. The suppression of hysteresis due to consecutive change of  $n$  is very improbable too. Therefore, the conductance hysteresis is rather robust in the region  $T_C < T_{\text{FE}} < T_C^0$ , however it is not very stable for  $T_{\text{FE}} < T_C$ .

#### D. SET with “slow” FE (dielectric) in the gate capacitor ( $t_{\text{FE}} \gg t_{\text{ex}}$ )

Characteristic time  $t_{\text{ex}}$  is the time between consecutive electron jumps to the grain. It depends on the gate voltage and it is comparable with  $t_d$  for weak Coulomb blockade.

The intermediate region,  $t_d \ll t_{\text{FE}} \ll t_{\text{ex}}$ , shows similar results for the conductance peak value as the region  $t_{\text{FE}} \gg t_{\text{ex}}$ . However, the peak shape in the intermediate region is quantitatively different since changing the gate voltage  $V_g$  the ratio  $t_{\text{FE}}/t_{\text{ex}}$  changes too. However, our calculations show that the difference in the shape of the peaks is not qualitative. Therefore it is difficult to observe it in an experiment. Thus, we consider both the intermediate and the “slow” FE regions simultaneously.

The limit of slow FE was studied before using the mean field theory. In particular, two different situations were discussed in Refs. [24,27]. In Ref. [27] the SET with linear dielectric material in the gate capacitor was discussed. It was shown that due to coupling of fast SET system with slow dielectric system the hysteresis of the conductance as a function of  $Q_0$  appears at large positive susceptibility of the dielectric layer ( $\chi_0 > \chi_0^{\text{cr}} = T_e C_\Sigma / (\pi C_g^0 (E_c + T))$ ). The Ref. [24] studied the SET with strongly non-linear FE material in the gate capacitor. Similar to the case of “fast” FE layer the hysteresis in the vicinity of the point  $Q_0 = 0$  was predicted. In the present paper we study the conductance behavior moving from “fast” to “slow” FE (dielectric) in the presence of FE (dielectric) polarization fluctuations. These fluctuations substantially modify the behavior of SET even in the case of “slow” FE.

Following the mean field theory of the SET with “slow” and weak dielectric layer ( $0 < \chi_0 < \chi_0^{\text{cr}}$ ) [24] in the gate capacitor the conductance in the vicinity of  $Q_0 = e/(2\epsilon_0)$  has the form

$$\sigma^{\text{MF}}/\sigma_0 \approx \frac{e\delta Q_0 / (C_\Sigma k_B T_e)}{\sinh(e\delta Q_0 / (C_\Sigma k_B T_e))} \approx 1 - \frac{1}{6} \left( \frac{e\delta Q_0}{C_\Sigma k_B T_e} \right)^2, \quad (18)$$

where  $\delta Q_0 = Q_0 - e/(2\epsilon_0)$ . Equation (18) is valid for small deviations  $\delta Q_0$ . The FE fluctuations lead to aver-

aging of the maximum over a finite region of  $Q_0$ . This region is proportional to the square root of the FE fluctuations dispersion,  $S_g \sqrt{D_P} \sim \sqrt{T_{\text{FE}}}$ . For equal temperatures  $T_{\text{FE}} = T_e = T$  the averaging gives the following maximum value for conductance

$$\begin{aligned} \sigma_{\text{max}}^{\text{av}} &= \sigma_0 \left( 1 - \frac{1}{18} \left( \frac{e S_g \sqrt{D_P}}{C_\Sigma k_B T} \right)^2 \right) = \\ &= \sigma_0 \left( 1 - \frac{1}{18} \frac{4\pi C_g^0 e^2 \chi}{C_\Sigma^2 k_B T} \right). \end{aligned} \quad (19)$$

Equation (19) shows that the averaging over fluctuations leads to the decrease of conductance peak value. Moreover, with decreasing the temperature the conductance peak value decreases. This unexpected behavior is related to the fact that fluctuations of FE polarization behaves as  $\sqrt{T}$  leading to the “strong”  $\sim \sqrt{T}$  free energy difference fluctuations. Below we will show that FE fluctuations also smear the hysteresis appearance for  $\chi_0 > \chi_0^{\text{cr}}$ .

#### E. Transition from “fast” to “slow” FE (dielectric)

The analytical consideration is difficult for  $t_{\text{FE}} \sim t_d$ . Therefore we use MC simulations to study this region.

##### 1. $T_{\text{FE}} > T_C^0$ .

In the case of “fast” FE (dielectric) the conductance appears as series of peaks as a function of the gate charge  $Q_0$ . Here we consider the case of linear FE (dielectric) response. In this case the period of peaks and height is constant and does not depend on  $Q_0$ . The peak height is defined by an effective additional Coulomb blockade. In the case of “slow” FE (dielectric) the conductance is also a periodic function of  $Q_0$  (see Refs. [24,27]) with the same period as in the case of “fast” dielectric. However, the shape of conductance peaks strongly depends on the magnitude of the dielectric susceptibility,  $\chi_0$ . For large susceptibility the conductance shows hysteresis behavior as a function of  $Q_0$  while for small susceptibility the hysteresis is absent. The hysteresis behavior was demonstrated in Refs. [24,27] using the mean field theory in the absence of fluctuations of the FE (dielectric) polarization. Our numerical simulations show that FE fluctuations destroy the hysteresis for temperatures  $T_{\text{FE}} = T_e = T$ . Lowering the FE temperature  $T_{\text{FE}}$  decreases the fluctuations of  $Q_0$  but the hysteresis width also decreases with electronic temperature  $T_e$ . Therefore to observe the hysteresis in the case of “slow” dielectric it is necessary to use the SET with different temperatures of the dielectric layer and the current conducting circuit,  $T_{\text{FE}} < T_e$ .

Figure 9 shows the evolution of function  $\sigma(Q_0)$  with increasing parameter  $\gamma$  for large susceptibility  $\chi_0$  for the following parameters:  $C_g^0 = 0.03 C_\Sigma$ ,  $\alpha_P = 0.5$ ,

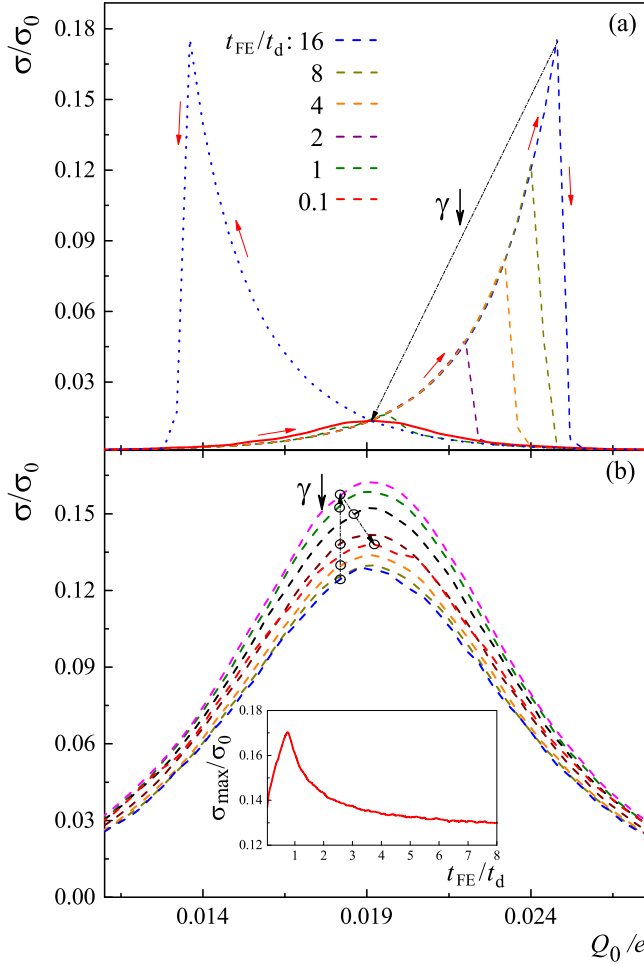


FIG. 9. (Color online) Conductance of SET as a function of  $Q_0$  for different  $t_{FE}$ . (a) FE fluctuations are absent ( $T_{FE} \ll T_e$ ). Red arrows show the path around the hysteresis loop. Both hysteresis branches are shown for  $t_{FE}/t_d = 16$ . (b) FE fluctuations are present ( $T_{FE} = T_e$ ). Inset in the panel (b) shows the dependence of the peak value of the conductance on  $t_{FE}$ .

$e^2\tilde{\beta}_P = 3 \cdot 10^{-4}$ ,  $T_e = 0.06E_c$ . Panel (a) shows the ideal case in the absence of FE fluctuations and temperatures  $T_{FE} \ll T_e$ . For large FE relaxation time,  $t_{FE} \gg t_d$ , the hysteresis is very pronounced, see blue dashed and blue dotted lines. Red solid arrows show the path around the hysteresis loop. The hysteresis width and the maximum value of conductance decrease with decreasing time  $t_{FE}$  ( $\gamma$ ). For  $t_{FE} \ll t_d$  the hysteresis disappears and the conductance is suppressed due to an additional Coulomb blockade effect. The situation is very different for finite FE fluctuations and temperatures  $T_{FE} = T_e$ , see panel (b). In this case the conductance hysteresis is absent for  $t_{FE} \gg t_d$ . The conductance as a function of  $Q_0$  has a peak in the vicinity of  $\epsilon_0 Q_0 = e/2$ . The peak value has a non-monotonic behavior with  $t_{FE}$ . The inset in panel (b) shows the conductance peak value,  $\sigma_{max} = \sigma|_{\epsilon_0 Q_0 = e/2}$ , as a function of  $t_{FE}$ . The curve has a peak at  $t_{FE} \approx t_d$ .

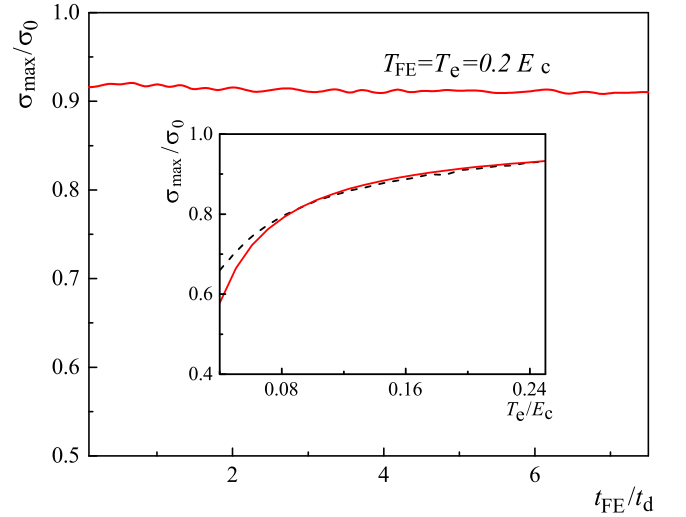


FIG. 10. (Color online) Conductance peak value vs.  $t_{FE}$  for small FE (dielectric) susceptibility,  $\chi_0$ . The inset shows the conductance peak value at  $t_{FE}/t_d = 8$  as a function of temperature  $T_e = T_{FE}$ . Dashed black line shows the result of MC simulations. Red solid line corresponds to the modified Eq. (19).

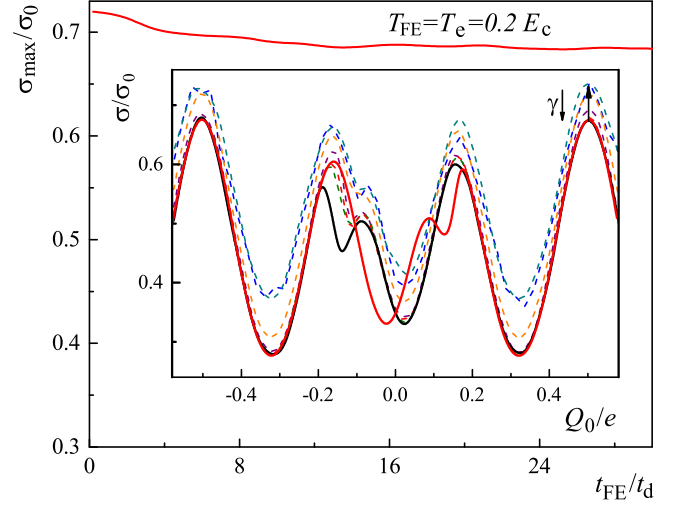


FIG. 11. (Color online) Conductance,  $\sigma_{max} = \sigma|_{Q_0=e/2}$ , vs.  $t_{FE}$  for negative susceptibility,  $\chi_0$ , ( $T_e = T_{FE} < T_c^0$ ). Inset: conductance of SET as a function of  $Q_0$  for different  $t_{FE}$ . Red solid curve stands for increasing  $Q_0$ . All other curves stand for decreasing  $Q_0$ . Solid red and black lines are for  $t_{FE} \gg t_d$ . Blue dashed line shows the opposite case,  $t_{FE}/t_d = 0.1$ . All other curves correspond to intermediate  $t_{FE}$ .

If susceptibility,  $\chi_0$ , is small and the hysteresis is absent at  $t_{FE} \gg t_d$ , the conductance is a periodic function of  $Q_0$  (in the absence of non-linear term in Eq. (4)). Figure 10 shows the dependence of the peak value of the conductance,  $\sigma_{max} = \sigma|_{\epsilon_0 Q_0 = e/2}$ , on the FE relaxation time,  $t_{FE}$ . The curves in Fig. 10 are plotted in the presence of FE fluctuations for the following parameters:  $\alpha_P = 2$ ,

$C_g^0 = 0.01 C_\Sigma$ ,  $T_e = T_{FE} = 0.2E_c$ . One can see that in this case the peak value does not depend on the FE relaxation time,  $t_{FE}$ . The inset in Fig. 10 shows the dependence of the conductance peak value on temperature for time  $t_{FE} \gg t_d$ , see the black dashed line. The peak value increases with temperature. It is in a qualitative agreement with Eq. (19). The red line in the inset shows the same function as in Eq. (19), however with different coefficient (1/7) instead of (1/18). All curves in the inset are plotted for fixed susceptibility,  $\chi_0$ .

## 2. $T_{FE} < T_C^0$ .

Above we have shown that for “fast” FE the conductance has hysteresis as a function of  $Q_0$ . Our MC simulations show that this hysteresis exists even for “slow” FE. The hysteresis is robust against the FE fluctuations (see red and black lines in the inset in Fig. 11). Inset in Fig. 11 shows the SET conductance versus the gate charge  $Q_0$  and the FE relaxation time  $t_{FE}$  in the presence of FE polarization fluctuations for the following parameters:  $C_g^0 = 0.2 C_\Sigma$  and  $T_e = T_{FE} = 0.2E_c$ ,  $\alpha_P = -2$ ,  $e^2\tilde{\beta}_P = 0.13$ . The conductance peak value decreases with increasing the FE relaxation time (see the curve in Fig. 11).

## F. Discussion of some experimental problems

The important question about implementation of the SET with FE layer in the gate capacitor is related to the FE Curie temperature. This temperature and the dielectric permittivity decrease with decreasing the FE layer thickness [48,49]. A critical thickness exists for most of FE materials. Below this thickness the FE phase transition does not exist ( $T_C^0$  becomes negative). Moreover, boundary conditions at the FE layer surface in the SET also contribute to the degradation of FE properties. Since the grain voltage is not fixed the FE internal electric field is not screened effectively leading to the reduction of the FE temperature and dielectric permittivity. The question about electric properties of FE material confined in such a small volume is currently open. In our consideration we assume FEs with low Curie temperature. One example is TTF-CA FE material. Bulk TTF-CA under the close circuit boundary conditions has Curie temperature,  $T_C^0 = 80$  K [46,50]. For this FE material  $T_C^0$  can be of order of  $(0.1 - 0.2)E_c$ . In Ref. [51] TTF-CA film was confined at one surface with a granular film. Therefore there was no effective screening of the internal FE field. In this system the FE Curie temperature has lower value  $T_C^0 = 50$  K.

For Coulomb blockade effects to exist at such a high temperature ( $\sim 50$  K) it is necessary to produce a rather small island in the SET with a size of approximately 5 nm. Assuming that the insulator thickness in the tunnel junctions is about 1 nm and  $\epsilon_{jun} \approx 5$  we find,

$C \sim 10^{-18}$  F. Usually, the resistance of the tunnelling junction is about  $10^6$  Ohm leading to the discharging time  $t_d \sim 10^{-12}$  s. Using tunnel junctions with resistance  $\sim 10^7$  Ohm one can increase the FE discharging time to  $t_d \sim 10^{-11}$  s.

It is known that dielectric relaxation time in materials depends on the mechanism of dielectric response. Two groups of materials are most promising for our purposes. In the first group the dielectric response is caused by the elastic mechanisms. The electronic mechanism does not produce a very high dielectric permittivity, instead it gives a very fast response with  $t_{FE} \sim 10^{-15}$  s. Usual insulators such as Si, SiO<sub>2</sub> and Al<sub>2</sub>O<sub>3</sub> have such a response mechanism. These materials can not be used as “retarded” in a SET. A SET with these insulators can be described using “classical” theory. The ionic elastic mechanism gives a higher dielectric permittivity but slower response with  $t_{FE} \sim 10^{-11} - 10^{-14}$  s. This mechanism substantially contributes to the dielectric response of semiconductors (GaAs and CdS) and ionic crystals such as NaCl. Insulators with this type of dielectric response can be used to investigate the limits  $t_{FE} \ll t_d$  and  $t_{FE} \sim t_d$ . Second group of materials have thermal mechanisms of dielectric response. These mechanisms give a rather high permittivity but longer relaxation time,  $t_{FE} \sim 10^{-4} - 10^{-10}$  s. Moreover, relaxation time in these materials increases with decreasing temperature. The dielectric response of relaxor FEs (such as PMN-PSN [52] with  $t_{FE} \sim 10^{-9}$  s at room temperature) are usually due to thermal mechanism. These materials can be considered as slow FEs with  $t_{FE} \gg t_d$ .

Most FEs materials are rather slow with dielectric relaxation time well below 1 THz. This is due to ionic nature of their dielectric response. However, recently new types of electronic FEs were discovered. One of them is TTF-CA. This material has dielectric relaxation time in the THz region [47]. This material can be used to study interaction of SET with retarded FEs.

## IV. CONCLUSION

We studied the SET with a FE or a dielectric placed in the gate capacitor. In contrast to the previous papers, we investigated the system behavior for arbitrary ratio between the FE relaxation time,  $t_{FE}$ , and the SET characteristic time,  $t_d$ . We used analytical methods and Monte-Carlo simulations to study the SET behavior.

We considered the case of “fast” FE (dielectric) with  $\hbar/E_c \ll t_{FE} \ll t_d$ . We showed that this case is different from the “classical” SET theory, where the instant response,  $\hbar/E_c \gg t_{FE}$ , of dielectric material is assumed. Thus, “fast” FE has the retarded response. We showed that retarded FE (dielectric) response leads to the appearance of an additional contribution to the Coulomb blockade effect and suppresses the SET conductance. The conductance as a function of the gate charge  $Q_0$  behaves differently at different temperatures. Below

a certain temperature  $T_C^0$  (which is the Curie temperature of the FE inside the gate capacitor) the conductance shows the hysteresis behavior. Above  $T_C^0$  no hysteresis appears in the case of “fast” FE. Monte-Carlo simulations allowed us to take into account fluctuations of the FE (dielectric) polarization. For “fast” FE these fluctuations partially suppress the additional Coulomb blockade effect. We showed that conductance hysteresis is robust against these fluctuations.

We studied the case of “slow” FE (dielectric),  $t_{FE} \gg t_d$ . This limit was discussed in literature using the mean field approach in the past. The interesting feature is related to the fact that due to coupling of fast SET subsystem with slow FE subsystem the conductance of the SET showed the hysteresis behavior even for temperatures,  $T > T_C^0$ . Thus, the nature of hysteresis is not related to the spontaneous polarization of the FE layer and may appear even with simple dielectric being placed in the gate capacitor. We used Monte-Carlo simulations to re-investigate this case. We found that FE (dielectric) fluctuations suppress the hysteresis. The only way to observe this hysteresis is to produce the FE (dielectric) layer temperature lower than the temperature of electrons in the SET leads (source and drain) and the island, ( $T_{FE} \ll T_e$ ).

We showed that for “slow” FE and low temperature,  $T < T_C^0$ , the SET conductance as function of the gate charge  $Q_0$  shows the hysteresis due to FE instability.

This hysteresis is robust against FE fluctuations.

Using the Monte-Carlo simulations we studied the transitional region between “fast” and “slow” FE. The transition depends on temperature (or the susceptibility of the FE (dielectric) layer). At high temperatures (low susceptibility) the peak value of the SET conductance is almost independent of the FE relaxation time. For temperatures close to  $T_C^0$  (high susceptibility) the conductance peak value non-monotonically depends on the FE relaxation time. A maximum appears close to  $t_{FE} = t_d$ . Below the Curie point ( $T < T_C^0$ ) the conductance peak value decreases with increasing  $t_{FE}$ .

## V. ACKNOWLEDGEMENTS

I. B. was supported by NSF under Cooperative Agreement Award EEC-1160504, NSF PREM Award and the U.S. Civilian Research and Development Foundation (CRDF Global). N. C. and S. F. are grateful to Russian Academy of Sciences for the access to JSCC and Uran clusters and Kurchatov center for access to HCP supercomputer cluster. S. F. acknowledges support of the Russian foundation for Basic Research (grant No. 13-02-00579). N. C. acknowledges Russian Science Foundation (grant No. 14-12-01185) for support of supercomputer simulations.

- 
- <sup>1</sup> F. Giazotto, *Nature Phys.* **11**, 527 (2015).  
<sup>2</sup> D. J. van Woerkom, A. Geresdi, and L. P. Kouwenhoven, *Nature Phys.* **11**, 547 (2015).  
<sup>3</sup> Z.-Z. Li, C.-H. Lam, and J. Q. You, *Scientific Reports* **5**, 11416 (2015).  
<sup>4</sup> I. M. Khaimovich, J. V. Koski, O. P. Saira, V. E. Kravtsov, and J. P. Pekola, *Nature Communications* **6**, 7010 (2015).  
<sup>5</sup> K. Horibe, T. Kodera, and S. Oda, *Appl. Phys. Lett.* **106**, 053119 (2015).  
<sup>6</sup> M. R. Islam, D. Joung, and S. I. Khondaker, *Nanoscale* **7**, 9786 (2015).  
<sup>7</sup> P. Hakkinen, A. Isacsson, A. Savin, J. Sulkko, and P. Hakkonen, *Nano Lett.* **15**, 1667 (2015).  
<sup>8</sup> P. Strasberg, G. Schaller, T. Brandes, and M. Esposito, *Phys. Rev. Lett.* **110**, 040601 (2013).  
<sup>9</sup> A. V. Feshchenko, J. V. Koski, and J. P. Pekola, *Phys. Rev. B* **90**, 201407(R) (2014).  
<sup>10</sup> P. G. Kirton and A. D. Armour, *Phys. Rev. B* **87**, 155407 (2013).  
<sup>11</sup> K. K. Likharev, N. S. Bakhvalov, G. S. Kazacha, and S. I. Serdyukova, *IEEE Trans. Magn.* **25**, 1436 (1989).  
<sup>12</sup> D. V. Averin and K. K. Likharev, *Journal of Low Temperature Physics* **62**, 345 (1986).  
<sup>13</sup> L. Y. Gorelik, A. Isacsson, M. V. Voinova, B. Kasemo, R. I. Shekhter, and M. Jonson, *Phys. Rev. Lett.* **80**, 4526 (1998).  
<sup>14</sup> A. D. Armour and A. MacKinnon, *Phys. Rev. B* **66**, 035333 (2002).  
<sup>15</sup> T. Nord, L. Y. Gorelik, R. I. Shekhter, and M. Jonson, *Phys. Rev. B* **65**, 165312 (2002).  
<sup>16</sup> T. Novotny, A. Donarini, and A.-P. Jauho, *Phys. Rev. Lett.* **90**, 256801 (2003).  
<sup>17</sup> N. M. Chtchelkatchev, W. Belzig, and C. Bruder, *Phys. Rev. B* **70**, 193305 (2004).  
<sup>18</sup> A. D. Armour, M. P. Blencowe, and Y. Zhang, *Phys. Rev. B* **69**, 125313 (2004).  
<sup>19</sup> A. D. Armour, *Phys. Rev. B* **70**, 165315 (2004).  
<sup>20</sup> D. A. Rodrigues, J. Imbers, and A. D. Armour, *Phys. Rev. Lett.* **98**, 067204 (2007).  
<sup>21</sup> C. B. Doiron, W. Belzig, and C. Bruder, *Phys. Rev. B* **74**, 205336 (2006).  
<sup>22</sup> R. Hussein, A. Metelmann, P. Zedler, and T. Brandes, *Phys. Rev. B* **82**, 165406 (2010).  
<sup>23</sup> S. A. Fedorov, A. E. Korolkov, N. M. Chtchelkatchev, O. G. Udalov, and I. S. Beloborodov, *Phys. Rev. B* **90**, 195111 (2014).  
<sup>24</sup> S. A. Fedorov, A. E. Korolkov, N. M. Chtchelkatchev, O. G. Udalov, and I. S. Beloborodov, *Phys. Rev. B* **89**, 155410 (2014).  
<sup>25</sup> J. P. Pekola, J. J. Vartiainen, M. Mottonen, O.-P. Saira, M. Meschke, and D. V. Averin, *Nature Physics* **4**, 120 (2014).  
<sup>26</sup> B. A. Strukov and A. P. Levanyuk, *Ferroelectric Phenomena in Crystals* (Springer, Geidelberg, 1998, 1998).  
<sup>27</sup> S. A. Fedorov, N. M. Chtchelkatchev, O. G. Udalov, and I. S. Beloborodov, *Phys. Rev. B* **92**, 115425 (2015).

- <sup>28</sup> L. R. C. Fonseca, A. N. Korotkov, K. K. Likharev, and A. A. Odintsov, *J. Appl. Phys.* **78**, 3238 (1995).
- <sup>29</sup> H.-S. Goan, *Phys. Rev. B* **70**, 075305 (2004).
- <sup>30</sup> D. Mozyrsky, I. Martin, and M. B. Hastings, *Phys. Rev. Lett.* **92**, 018303 (2004).
- <sup>31</sup> C. Waahuber and H. Kosina, *IEEE Trans. Computer-Aided Design of Integrated Circuits and Systems* **16**, 937 (1997).
- <sup>32</sup> J. Bylander, T. Duty, and P. Delsing, *Nature* **434**, 361 (2005).
- <sup>33</sup> F. Giazotto, T. T. Heikkila, A. Luukanen, A. M. Savin, and J. P. Pekola, *Rev. Mod. Phys.* **78**, 217 (2006).
- <sup>34</sup> A. N. Korotkov, M. R. Samuelsen, and S. A. Vasenko, *J. Appl. Phys.* **76**, 3623 (1994).
- <sup>35</sup> O.-P. Saira, M. Meschke, F. Giazotto, A. M. Savin, M. Mottonen, and J. P. Pekola, *Phys. Rev. Lett.* **99**, 027203 (2007).
- <sup>36</sup> S. Lefevre, S. Volz, and P.-O. Chapuis, *International Journal of Heat and Mass Transfer* **49**, 251 (2006).
- <sup>37</sup> K. L. Grosse, M.-H. Bae, F. Lian, E. Pop, and W. P. King, *Nature Nanotechnology* **6**, 287 (2011).
- <sup>38</sup> J. B. Khurgin, *Phys. Rev. Lett.* **98**, 177401 (2007).
- <sup>39</sup> Y.-S. Liu, B. C. Hsu, and Y.-C. Chen, *J. Phys. Chem. C* **115**, 6111 (2011).
- <sup>40</sup> L. D. Landau and E. Lifshitz, *Course of Theoretical Physics: Vol.: 8: Electrodynamics of Continuous Media* (Pergamon Press, 1960).
- <sup>41</sup> R. Zwanzig, *J. Stat. Phys.* **9**, 215 (1973).
- <sup>42</sup> M. Bixon and R. Zwanzig, *J. Stat. Phys.* **3**, 245 (1973).
- <sup>43</sup> M. H. Devoret, D. Esteve, H. Grabert, G. L. Ingold, H. Pothier, and C. Urbina, *Phys. Rev. Lett.* **64**, 1824 (1990).
- <sup>44</sup> S. M. Girvin, L. I. Glazman, M. Jonson, D. R. Penn, and M. D. Stiles, *Phys. Rev. Lett.* **64**, 3183 (1990).
- <sup>45</sup> M. Devoret and H. Grabert, *Single Charge Tunneling*, Vol. 264 (New York, Plenum, 1992).
- <sup>46</sup> K. Kobayashi, S. Horiuchi, R. Kumai, F. Kagawa, Y. Murakami, and Y. Tokura, *Phys. Rev. Lett.* **108**, 237601 (2012).
- <sup>47</sup> T. Miyamoto, H. Yada, H. Yamakawa, and H. Okamoto, *Nature Communications* **4**, 2586 (2013).
- <sup>48</sup> V. M. Fridkin, *Phys. Usp.* **49**, 193 (2006).
- <sup>49</sup> V. M. Fridkin, R. V. Gaynutdinov, and S. Ducharme, *Phys. Usp.* **53**, 199 (2010).
- <sup>50</sup> M. Buron-LeCointe, M. H. Lemee-Cailleau, H. Cailleau, S. Ravy, J. F. Berar, S. Rouziere, E. Elkaim, , and E. Collet, *Phys. Rev. Lett.* **96**, 205503 (2006).
- <sup>51</sup> M. Huth, A. Rippert, R. Sachser, and L. Keller, *Materials Research Express* **1**, 046303 (2014).
- <sup>52</sup> R. Grigalaitis, J. Banyas, J. Macutkevicius, R. Adomavicius, A. Krotkus, K. Bormanis, and A. Sternberg, *Journal of the European Ceramic Society* **30**, 613 (2010).